Quantum Fluctuations and Coherence in High-Precision Single-Electron Capture

Vyacheslavs Kashcheyevs and Janis Timoshenko

Faculty of Computing and Faculty of Physics and Mathematics, University of Latvia, LV-1586, Riga, Latvia

(Received 17 May 2012; published 20 November 2012)

The phase of a single quantum state is undefined unless the history of its creation provides a reference point. Thus, quantum interference may seem hardly relevant for the design of deterministic single-electron sources which strive to isolate individual charge carriers quickly and completely. We provide a counter-example by analyzing the nonadiabatic separation of a localized quantum state from a Fermi sea due to a closing tunnel barrier. We identify the relevant energy scales and suggest ways to separate the contributions of quantum nonadiabatic excitation and back tunneling to the rare noncapture events. In the optimal regime of balanced decay and nonadiabaticity, our simple electron trap turns into a single-lead Landau-Zener back tunneling interferometer, revealing the dynamical phase accumulated between the particle capture and leakage. The predicted ''quantum beats in back tunneling'' may turn the error of a single-electron source into a valuable signal revealing essentially nonadiabatic energy scales of a dynamic quantum dot.

DOI: 10.1103/PhysRevLett.109.216801 PACS numbers: 73.63.Kv, 73.21.La, 73.23.Hk

Successful demonstration of electron-on-demand sources based on electrostatic modulation of nanoelectronic circuit elements such as dynamic quantum dots [1–3] or mesoscopic capacitors [4,5] has offered a prospect of building an electronic analog of few-photon quantum optics [6] that exploits the particle-wave duality and entanglement of individual elementary excitations in a Fermi sea [7–10]. This ambitious goal is complemented by a long-standing challenge in quantum metrology [11] to untie the definition of ampere from the mechanical units of the International System of Units [12] and implement a current standard based on direct counting of discrete charge carriers. Thus far the overlap between these research directions [13,14] has been rather limited arguably because metrological applications strive to maximize the particle nature of on-demand excitations. Optimizing the trade-off between speed and accuracy of single-electron isolation [2] does require consideration of quantum error mechanisms such as nonadiabatic excitation [15–17] or back tunneling [18–21]. However, these effects have been hard to differentiate experimentally owing to the complexity of nonequilibrium many-particle quantum dynamics [22] and experimental challenges in exercising high-speed control of the electrostatic landscape. The quantum phase of the captured particle has been considered thus far as inconsequential for accuracy and inaccessible for measurement unless the particle is ejected into a separate interferometer [10].

In this Letter, we propose a new type of interferometry to measure and thus control the nonequilibrium energy scales governing the decoupling of a dynamic quantum dot from a Fermi sea. Remarkably, our approach requires neither multiple spatial paths [9,10] nor noise measurements [8,22,23], relying instead on quantum beats in spontaneous emission of electrons back to the source lead. Using a generic [22,24] effective single-particle model we predict an interference pattern in the charge capture probability that reflects the dynamical quantum phase accumulated between the isolation of the localized quantum state and the onset of back tunneling.

Our innovations can be explained within a simple two-path picture of Mach-Zehnder interferometry in a time domain; see Fig. 1(a). The first branch is quantum excitation above the Fermi edge in the source lead due to the finite time scale τ for the pinch-off of tunneling [16] [see dark gray arrows in Fig. 1(a)]. The corresponding energy spread and the (small) path-splitting amplitude can be estimated by the energy-time uncertainty, $\Gamma_c \equiv \hbar/(\pi\tau)$, and the Landau-Zener theory [25], respectively. The second branch is adiabatic lifting of the occupied energy level followed by splitting of a small amplitude back into the lead once the level emerges above the Fermi sea [see light

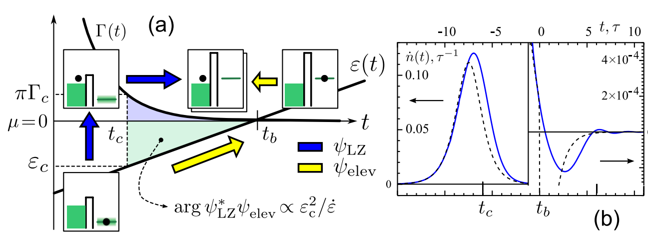

FIG. 1 (color online). (a) Schematic plot of the rising level energy $\varepsilon(t)$ and exponentially decreasing broadening $\Gamma(t)$. Pictograms illustrate the two paths for interference: dark gray (blue) arrows mark nonadiabatic excitation followed by phase accumulation above the Fermi edge μ; light gray (yellow) arrows show adiabatic ''elevator ride'' and back tunneling. (b) Instantaneous current flowing into the quantum dot, $\dot n(t)$. Thick (blue) line, exact Eq. (3); thin dashed line, quantum-broadened Markov approximation, Eq. (4). Model parameters are $\varepsilon_c/\Delta_{\rm ptb} = -6$, $\Gamma_c/\Delta_{\rm ptb} = 1.2$, $T = 0$.

gray arrows in Fig. 1(a)]. This elevation and back tunneling branch is sensitive to electrostatic cross coupling between the barrier and the bottom of the confining potential well; we quantify this cross talk by the *plunger-to-barrier* ratio $\Delta_{\rm ptb} \equiv \dot{\varepsilon}\tau$ (shift of the localized energy level ε during the characteristic decoupling time). The output ports of the interferometer can be read either by detecting excitations created in the Fermi sea, or, more conveniently, by measuring the charge capture probability. The latter is accessible in experiment by repeated ejection of the captured electrons into a collector lead and measuring the resulting dc current [1,2,14,19–21]. The beam splitters are tuned by $\Delta_{\rm ptb}/\Gamma_c$ to maximize contrast, the phase measurement reveals the "elevator speed" $\dot{\varepsilon} \propto \Delta_{\rm ptb}\Gamma_c$, and the temperature smearing allows absolute calibration of the energy scales. Our scheme is conceptually related to Landau-Zener-Stückelberg interferometry [26–28] which measures the relative dynamical phase of discrete states via creation of superposition in sequential nonadiabatic level crossings. In contrast, we propose to access the phase of a *single* localized state measured against a reference point in the continuum (defined by a sufficiently fast decoupling and a sharp Fermi edge).

The proposed measurement addresses a persistent challenge in robust utilization of electrostatically defined quantum dot devices: control of rate (τ), type (barrier versus plunger), and magnitude ($\Delta_{\rm ptb}$) at which external voltage pulses are converted into the time-dependent potential guiding individual transport electrons on the chip. Although parametric time dependency of the electronic matrix elements is the standard input for theory [24,29], in practice mesoscopic fluctuations (due to distribution and charge switching dynamics of impurities, finite fabrication precision, etc.) and challenges of signal propagation at high frequencies (GHz range) often require measuring the characteristic quantities on a sample-to-sample basis. For near-equilibrium, bias spectroscopy [30] provides a versatile tool, but for the large-amplitude, high-frequency modulation the options are limited [1]. As a foreseeable direct application of our results we expect a reliable measurement of $\Gamma_c/\Delta_{\rm ptb}$ to help settle the debate on the fundamental factors limiting the precision of the state-of-the-art single-electron-based current sources [2]. More generally, we hope our analysis will facilitate the crossover of ideas between fundamental and applied directions of single electronics.

Model and formalism.—The model is described by an effective single-particle Hamiltonian $\mathcal{H} = \varepsilon(t)d^\dagger d + \sum_k\{\epsilon_k c_k^\dagger c_k + V(t)[c_k^\dagger d + d^\dagger c_k]\}$, where $d^\dagger$ creates a localized nondegenerate electronic state in the dot and $c_k^\dagger$ creates a quasicontinuous state in the lead. The lead is connected to a thermal reservoir with chemical potential $\mu = 0$ and temperature T. Employing a time-dependent tunneling Hamiltonian relies on time scale separation [24]: fast screening in the leads determines the instantaneous values of the slowly varying parameters for the underscreened region (the quantum dot). We choose k-independent real V and the wideband limit so that $\Gamma(t) \equiv 2\pi\rho V^2(t)$ and $\varepsilon(t)$ are the fully dressed elastic width and the on-site energy, respectively (ρ is the density of states in the lead).

The quantum kinetic equation for the average occupation within the model, $n(t) \equiv \langle d^\dagger(t)d(t)\rangle$, is given by the nonequilibrium Green functions theory [24],

$$\hbar\dot{n}(t) = -\Gamma(t)n(t) - \int\frac{f(\epsilon)}{\pi\hbar}\,\mathrm{Im}\int_{-\infty}^{t}\sqrt{\Gamma(t)\Gamma(t')}G(t,t')e^{i\epsilon(t-t')/\hbar}dt'd\epsilon, \tag{1}$$

where $f(\epsilon)$ is the Fermi distribution and $G(t,t')$ is the retarded Green function of the level,

$$G(t,t') = -i\Theta(t-t')e^{-i\int_{t'}^{t}dt_1[\varepsilon(t_1)-i\Gamma(t_1)/2]/\hbar}. \tag{2}$$

Integrating Eq. (1) gives [cf. Eq. (44) of Ref. [24]]

$$n(t) = \int\frac{f(\epsilon)}{2\pi\hbar^2}\left|\int_{-\infty}^{t}dt'G(t,t')\sqrt{\Gamma(t')}e^{-i\epsilon t'/\hbar}\right|^2 d\epsilon. \tag{3}$$

Equation (3) is the sum of probabilities to be scattered into the localized state from an occupied state in the continuum; one can show [31–33] that it agrees with the Floquet formalism [29,34] which is often used in the scattering form to study single-charge emitters [23,35,36]. In this work we consider electron trapping achieved by reducing $\Gamma(t)$ to zero as $t \to \infty$ and compute the capture probability $n_f \equiv \lim_{t\to\infty} n(t)$.

The history of parametric time dependence that affects $n(t)$ is limited by a finite memory time $\tau_{\rm mem} \equiv \hbar\min\{(kT)^{-1}, \Gamma^{-1}(t)\}$ due to (a) lead-induced dephasing of the discrete state and (b) thermal smearing in the reservoir. One can show [33] that, for sufficiently slow processes, when $|\dot{\varepsilon}|\tau_{\rm mem}^2 \ll \hbar$ (no phase rotation) and $|\dot{\Gamma}|\tau_{\rm mem} \ll \Gamma$ (well-defined Γ), the exact kinetic equation (1) can be replaced by a (quantum broadened) Markov approximation,

$$\hbar\dot{n} = -\Gamma(t)\{n(t) - n_{\rm eq}[\varepsilon(t),\Gamma(t)]\}, \tag{4}$$

with parametrically defined standard equilibrium occupation, $n_{\rm eq}(\varepsilon,\Gamma) = (2\pi)^{-1}\int d\omega\Gamma f(\omega)/[(\omega-\varepsilon)^2 + \Gamma^2/4]$. Although Eq. (4) still permits strongly nonadiabatic scenarios [37], for the decoupling problem at hand $\tau_{\rm mem}$ diverges at zero temperature as $t \to \infty$; thus, we must use Eq. (3).

We define a crossover moment t_c as the earliest time from which the quantum phase of the level can be preserved, $\int_{t_c}^{+\infty}\Gamma(t)dt = \hbar$, and explore exponential time dependence [16] of $\Gamma(t)$ around t_c,

$$\Gamma(t) = \pi\Gamma_c e^{-(t-t_c)/\tau}, \tag{5}$$

accompanied by a linear shift of energy [19,20,22,37],

$$\varepsilon(t) = \varepsilon_c + \Delta_{\text{ptb}}(t - t_c)/\tau. \tag{6}$$

The shape of $\varepsilon(t)$ and $\Gamma(t)$ for $t \ll t_c$ as well as the initial conditions for Eq. (1) are irrelevant for n_f if the ansatz (5) holds from a few τ before t_c. Whether the last particle exchange between the dot and the source (most likely to occur around $t \approx t_c$) results in a captured electron ($n_f \approx 1$) or a hole ($n_f \approx 0$) depends on the position of ε_c with respect to μ (below or above, respectively).

Experimental realization.—A prototypical realization for the model is a small near-empty electrostatically defined quantum dot with large level spacing and charging energy, as in, e.g., [3,17]. A linear ramp of voltage $\mathcal{V}_1(t)$ on a gate that defines the tunnel barrier between the source and the quantum dot creates the time dependencies (5) and (6) while a static voltage $\mathcal{V}_2$ on another gate can be used to tune the decoupling energy, $\varepsilon_c = -\alpha\mathcal{V}_2\Delta_{\text{ptb}} + \text{const.}$ $\Gamma_c \sim \tau^{-1}$ is inversely proportional to the rise time of the $\mathcal{V}_1(t)$ pulse.

Once $\Gamma(t)$ becomes negligible ($t \to \infty$ in our model), further modulation of the confining potential can ensure complete ejection of the captured electrons into the drain lead [2,21]. Repeating the whole cycle with a frequency $f \ll \tau^{-1}$ and measuring the dc component of the source-drain pumping current $I(\mathcal{V}_2)$ can provide accurate data on $n_f(\varepsilon_c) = I/(ef)$ (here e is the electron charge). Note that α is the fitting parameter [2,20,38] of the decay cascade model [21]; see Eq. (8c).

Qualitative picture.—The essential features of the model can be seen in the time-dependent ensemble-average current $\dot{n}(t)$ for $\Delta_{\text{ptb}} \approx \Gamma_c$ and $\epsilon_c < -\Delta_{\text{ptb}}$ at low temperature; see Fig. 1(b). Before the formation of the localized level, at times $t \ll t_c - \tau \ln|\epsilon_c|/\Gamma_c$, the average occupation number remains constant and equal to the average density of electrons per quantum state in the lead (1/2 in our dispersionless model). A large peak in the current near t_c marks adiabatic filling of the rapidly narrowing level. A much smaller opposite sign feature indicates the onset of back tunneling at $t > t_b$ with t_b defined by $\varepsilon(t_b) = \mu$. It is instructive to contrast the exact $\dot{n}(t)$ with the solution of the Markov equation (4) shown by the dashed line in Fig. 1(b). The level of agreement correlates with the condition $\Gamma(t) > \Gamma_c$ being fulfilled exponentially well for $t \ll t_c$, breaking down around t_c, and being strongly violated for $t > t_b$.

Probability of charge capture.—Our main result is

$$n_f = \int \frac{d\epsilon}{2\pi^2\Gamma_c} f(\epsilon) \left| \int_{-\infty}^{\infty} \exp\left[-\frac{x + e^{-x}}{2} + i\frac{\Delta_{\text{ptb}}}{2\pi\Gamma_c}\left(x - \frac{\epsilon - \varepsilon_c}{\Delta_{\text{ptb}}}\right)^2 \right] dx \right|^2. \tag{7}$$

$n_f(\varepsilon_c)$ is a steplike function changing from 1 to 0 as ϵ_c goes from $-\infty$ to $+\infty$. The limit forms are

$$n_f = f(\varepsilon_c), \qquad \Delta_{\text{ptb}}, \Gamma_c \to 0 \tag{8a}$$

$$n_f = (2/\pi)\tan^{-1} e^{-\varepsilon_c/\Gamma_c}, \qquad kT, \Delta_{\text{ptb}} \to 0 \tag{8b}$$

$$n_f = e^{-e^{\varepsilon_c/\Delta_{\text{ptb}}}}. \qquad kT, \Gamma_c \to 0 \tag{8c}$$

The limit (8a) corresponds to a sudden decoupling from equilibrium at $\varepsilon(t_c) = \varepsilon_c$, the corresponding step is symmetric under $\varepsilon_c \to -\varepsilon_c$ and maps out the thermal distribution [39]. The limit (8b) reproduces the result of Flensberg *et al.* [16], a symmetric step of width Γ_c. The double-exponential shape (8c) has been predicted previously [19–21] from a master equation and validated experimentally [2,38] with up to 10^{-6} relative accuracy. Our derivation reveals the plunger-to-barrier ratio Δ_{ptb} as the energetic measure of the step width.

Finite temperature is accounted for by simple thermal smearing, $n_f(\varepsilon_c) = \int n_f(\varepsilon_c - \epsilon)|_{T=0}(-\partial f/\partial\epsilon)d\epsilon$; thus, we focus mainly on $T = 0$. Figure 2 shows evolution of the line shape $n_f(\epsilon_c)$ as $\Gamma_c/\Delta_{\text{ptb}}$ is increased. The asymmetry around $\varepsilon_c = 0$ gets "inverted" with respect to the double-exponential (8c) at $\Gamma_c \approx 2\Delta_{\text{ptb}}$ before approaching the symmetric limit (8b). Nonperturbative asymptotics of Eq. (7) for $\epsilon_c \gg \max[\Delta_{\text{ptb}}, \Gamma_c]$ give an exponential dependence with a power-law prefactor,

$$n_f \sim \frac{2}{\pi}\left(\frac{2\epsilon_c}{\pi\Gamma_c}\right)^{\Delta_{\text{ptb}}/\Gamma_c} e^{-\varepsilon_c/\Gamma_c}, \qquad T \to 0, \tag{9}$$

shown in the log-scale inset of Fig. 2. This is similar to the Fermi function tail, $\sim e^{-\varepsilon_c/kT}$, which dominates the small-n_f asymptotics for $kT > \Gamma_c$ regardless of Δ_{ptb}. Thus, we conclude that both quantum and thermal fluctuations always trump the double-exponentially suppressed back tunneling for small n_f. This finding may have implications for the minimal slope position on the plateaus between successive current quantization steps in single-gate pumps [20,38]. A change in slope of $\log n_f$ versus ε_c

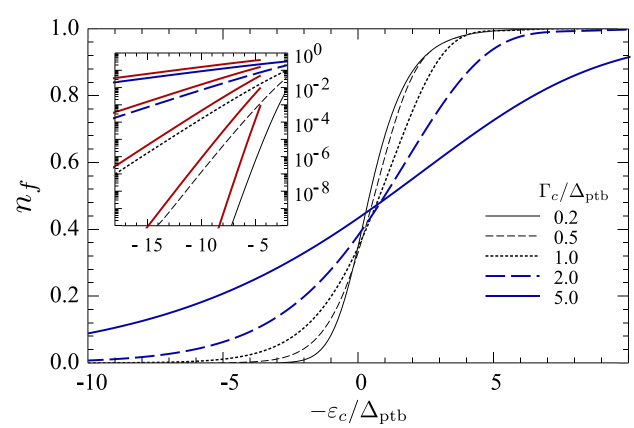

FIG. 2 (color online). Charge capture probability n_f as a function of the level energy ε_c at the decoupling moment. $T = 0$, and $\Gamma_c/\Delta_{\text{ptb}}$ is varied as indicated. The inset shows the same quantity in the logarithmic scale with additional thick (red) lines marking the asymptotics (9).

as the barrier-closing time scale τ is reduced may signal that $\Gamma_c/kT \gtrsim 1$, although this effect on its own would be hard to differentiate from local heating.

Quantum oscillations.—The asymptotics of $1 - n_f$ at large negative ε_c switches from $\sim e^{\varepsilon_c/\Delta_{\rm ptb}}$ to $\sim e^{\varepsilon_c/\Gamma_c}$ at $\Gamma_c = \Delta_{\rm ptb}$ via a surprising sequence of mini plateaus. The latter can be seen as ripples in the derivative $\partial n_f/\partial \varepsilon_c$, as shown in Fig. 3(a) and 3(b). Although the oscillation amplitude decays exponentially, the nonmonotonic behavior of $\partial n_f(\varepsilon_c)/\partial \varepsilon_c$ is manifest in the range of Γ_c from $0.8\Delta_{\rm ptb}$ to $2.2\Delta_{\rm ptb}$ at temperatures up to $kT \approx 0.35\Delta_{\rm ptb}$; see Fig. 3(c).

We interpret the oscillations as interference between two excitation paths that promote lead electrons above the Fermi energy. One path is capture, elevation, and back tunneling similar to elevator resonance activation proposed by Azbel' [40]. As seen from the scattering interpretation of Eq. (7), the electrons most likely to be captured have incoming energies $\epsilon \approx \varepsilon_c$; thus, we estimate the amplitude to be raised by an "elevator ride" from ε_c to an energy $\epsilon_e > \mu$ by a three-amplitude product,

$$\psi_{\rm elev}(\epsilon_e) \propto V(t_c) e^{-i\int_{t_c}^{t_e} \varepsilon(t)dt/\hbar} V(t_e), \qquad (10)$$

where the exit time $t_e > t_b$ is determined from $\varepsilon(t_e) = \epsilon_e$.

The other path from $\epsilon \approx \varepsilon_c$ to $\epsilon = \epsilon_e$ is Landau-Zener-like excitation due to the time dependence of $\Gamma(t)$. We estimate the corresponding amplitude by following the Landau solution of a two-level problem [25] with matrix elements $H_{11} = \epsilon_e$, $H_{22} = \varepsilon_c$, and $H_{12} = H_{21} = \Gamma(t)$ [41]. The adiabatic eigenvalues $E_1(t)$, $E_2(t)$ have a gap $\Delta E(t) = \sqrt{4\Gamma^2(t) + (\epsilon_e - \varepsilon_c)^2} > 0$ on the real axis but become degenerate if analytically continued into the complex t plane. The branching point of $E(t)$ with the smallest positive imaginary part, $t_0 = t_c + \tau \ln[2\Gamma_c/(\epsilon_e - \varepsilon_c)] + i\pi\tau/2$, determines the transition probability [25] $\exp[-2\,{\rm Im}\int_{{\rm Re}t_0}^{t_0} \Delta E(t)dt/\hbar] = \exp[-\pi\tau(\epsilon_e - \varepsilon_c)/\hbar]$.

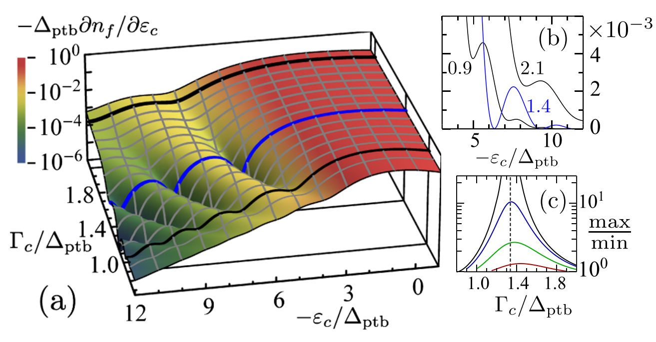

FIG. 3 (color online). (a) The derivative $-\Delta_{\rm ptb}\partial n_f/\partial \varepsilon_c$ (vertical axis, log scale) as a function of the decoupling energy ε_c and the ratio $\Gamma_c/\Delta_{\rm ptb}$ at $T = 0$. Three cuts at $\Gamma_c/\Delta_{\rm ptb} = 0.9$, 1.4, and 2.1 are shown on a linear scale in (b). (c) The ratio of the first interference maximum in $-\partial n_f(\varepsilon_c)/\partial \varepsilon_c$ to the first minimum on a log scale as a function of $\Gamma_c/\Delta_{\rm ptb}$ as $kT/\Delta_{\rm ptb}$ increases through 0, 0.1, 0.2, and 0.3 (from the topmost to the lowermost curve).

Neglecting preexponential and logarithmic terms, the amplitude for excitation at t_c and evolution up to t_e is

$$\psi_{\rm LZ}(\epsilon_e) \propto e^{-(\epsilon_e - \varepsilon_c)/(2\Gamma_c) - i\varphi_0} e^{-i\epsilon_e(t_e - t_c)/\hbar}, \qquad (11)$$

where φ_0 is the phase of the Landau-Zener transition (Stokes phase) known to depend weakly on energy [28].

We estimate the total noncapture probability as

$$1 - n_f \propto \int_{\mu=0}^{\infty} d\epsilon_e |\psi_{\rm LZ}(\epsilon_e) + \psi_{\rm elev}(\epsilon_e)|^2. \qquad (12)$$

The competition of $|\psi_{\rm LZ}|^2$ and $|\psi_{\rm elev}|^2$ at large negative ε_c agrees with the asymptotic envelope of n_f while ${\rm Re}\,\psi_{\rm LZ}(0)\psi^*_{\rm elev}(0)$ gives the oscillating part of $\partial n_f/\partial \varepsilon_c$,

$$e^{\varepsilon_c(\Delta_{\rm ptb}^{-1} + \Gamma_c^{-1})/2} \cos\left(\varphi_0 + \frac{\epsilon_c^2}{2\pi\Gamma_c\Delta_{\rm ptb}}\right). \qquad (13)$$

The argument of the cosine is the dynamical phase accumulated between t_c and t_b; see the shaded triangle in Fig. 1. Despite the crudeness of approximations leading to Eq. (13), the result agrees well with the exact solution Eq. (7) both in amplitude and phase, as shown in Fig. 4.

Feasibility.—The oscillation effect does not rely on any fine-tuning (apart from balancing the interferometer, $\Delta_{\rm ptb} \approx \Gamma_c$); thus, it should be robust against deviations from the assumed time dependencies. The most important foreseeable limitation is the overlap of additional interference modes which must be separated by a sufficiently large on-the-dot level spacing $\Delta\varepsilon$ from $t \approx t_c$ onward; our single-mode formula (7) is limited to $-\varepsilon_c < \Delta\varepsilon$ requiring $\Delta\varepsilon \gtrsim 8\Delta_{\rm ptb}$ to resolve the first interference minimum [33,42]. Using a recent Letter [17] on out-of-equilibrium excited states in a rapidly decoupling dynamic quantum dot, we read $\alpha = 0.28$ mV^{-1} from 100 MHz data in Fig. 1 of Ref. [17] and estimate the gap to the first exited state observed at 1 GHz to be $\Delta\varepsilon/\Delta_{\rm ptb} \approx 4.5$, which is the same

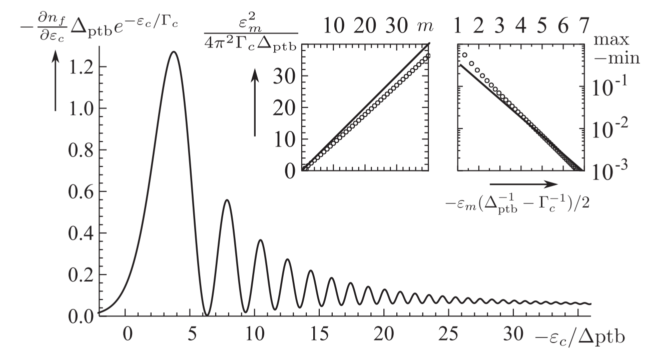

FIG. 4. Main panel: The derivative $-\partial n_f/\partial \varepsilon_c$ multiplied by $\Delta_{\rm ptb}e^{-\varepsilon_c/\Gamma_c}$ for $\Gamma_c/\Delta_{\rm ptb} = 1.4$ and $T = 0$. Left inset: The positions ε_m of the minima in the main graph versus their index number m scaled according to the two-path formula (13). Right inset: The absolute difference between a maximum and the preceding minimum of the oscillations shown in the main panel on a log scale versus a scaled $-\varepsilon_m$. The straight line of slope of ± 1 in both insets is plotted according to Eq. (13).

order of magnitude as our requirements. Measurements of a similar device [2] have just reached the required accuracy threshold for $n_f(\varepsilon_c)$, suggesting that the proposed dynamical phase interferometry is feasible with current technology.

Conclusions.—We have considered the quantum dynamics of isolating a single particle from a Fermi sea by a closing tunnel barrier and proposed ways to measure the relevant nonequilibrium energy scales. Time-domain interferometry revealing the dynamical phase of the confined particle offers an unexpected "built-in" instrument to quantify and separate the quantum effects hampering deterministic electron-on-demand operation which is a cornerstone for future on-the-chip electron quantum optics and a quantum realization of the ampere.

We thank Bernd Kaestner for discussions. This work has been supported by ESF Project No. 2009/0216/1DP/1.1.1.2.0/09/APIA/VIAA/044.

[1] M. D. Blumenthal, B. Kaestner, L. Li, S. Giblin, T. J. B. M. Janssen, M. Pepper, D. Anderson, G. Jones, and D. A. Ritchie, Nat. Phys. **3**, 343 (2007).
[2] S. P. Giblin, M. Kataoka, J. D. Fletcher, P. See, T. J. B. M. Janssen, J. P. Griffiths, G. A. C. Jones, I. Farrer, and D. A. Ritchie, Nat. Commun. **3**, 930 (2012).
[3] C. Leicht, P. Mirovsky, B. Kaestner, F. Hohls, V. Kashcheyevs, E. V. Kurganova, U. Zeitler, T. Weimann, K. Pierz, and H. W. Schumacher, Semicond. Sci. Technol. **26**, 055010 (2011).
[4] G. Fève, A. Mahé, J.-M. Berroir, T. Kontos, B. Plaçais, D. C. Glattli, A. Cavanna, B. Etienne, and Y. Jin, Science **316**, 1169 (2007).
[5] E. Bocquillon, F. D. Parmentier, C. Grenier, J.-M. Berroir, P. Degiovanni, D. C. Glattli, B. Plaçais, A. Cavanna, Y. Jin, and G. Fève, Phys. Rev. Lett. **108**, 196803 (2012).
[6] J.-W. Pan, Z.-B. Chen, C.-Y. Lu, H. Weinfurter, A. Zeilinger, and M. Żukowski, Rev. Mod. Phys. **84**, 777 (2012).
[7] A. Bertoni, P. Bordone, R. Brunetti, C. Jacoboni, and S. Reggiani, Phys. Rev. Lett. **84**, 5912 (2000).
[8] S. Ol'khovskaya, J. Splettstoesser, M. Moskalets, and M. Büttiker, Phys. Rev. Lett. **101**, 166802 (2008).
[9] J. Splettstoesser, M. Moskalets, and M. Büttiker, Phys. Rev. Lett. **103**, 076804 (2009).
[10] G. Haack, M. Moskalets, J. Splettstoesser, and M. Büttiker, Phys. Rev. B **84**, 081303(R) (2011).
[11] N. M. Zimmerman and M. W. Keller, Meas. Sci. Technol. **14**, 1237 (2003).
[12] M. J. T. Milton, J. M. Williams, and A. B. Forbes, Metrologia **47**, 279 (2010).
[13] T. Brandes, Phys. Rev. Lett. **105**, 060602 (2010).
[14] L. Fricke, F. Hohls, N. Ubbelohde, B. Kaestner, V. Kashcheyevs, C. Leicht, P. Mirovsky, K. Pierz, H. W. Schumacher, and R. J. Haug, Phys. Rev. B **83**, 193306 (2011).
[15] C. Liu and Q. Niu, Phys. Rev. B **47**, 13031 (1993).
[16] K. Flensberg, Q. Niu, and M. Pustilnik, Phys. Rev. B **60**, R16291 (1999).
[17] M. Kataoka, J. D. Fletcher, P. See, S. P. Giblin, T. J. B. M. Janssen, J. P. Griffiths, G. A. C. Jones, I. Farrer, and D. A. Ritchie, Phys. Rev. Lett. **106**, 126801 (2011).
[18] G. R. Aizǐn, G. Gumbs, and M. Pepper, Phys. Rev. B **58**, 10589 (1998).
[19] A. Fujiwara, K. Nishiguchi, and Y. Ono, Appl. Phys. Lett. **92**, 042102 (2008).
[20] B. Kaestner, C. Leicht, V. Kashcheyevs, K. Pierz, U. Siegner, and H. W. Schumacher, Appl. Phys. Lett. **94**, 012106 (2009).
[21] V. Kashcheyevs and B. Kaestner, Phys. Rev. Lett. **104**, 186805 (2010).
[22] J. Keeling, A. V. Shytov, and L. S. Levitov, Phys. Rev. Lett. **101**, 196404 (2008).
[23] F. D. Parmentier, E. Bocquillon, J.-M. Berroir, D. C. Glattli, B. Plaçais, G. Fève, M. Albert, C. Flindt, and M. Büttiker, Phys. Rev. B **85**, 165438 (2012).
[24] A.-P. Jauho, N. S. Wingreen, and Y. Meir, Phys. Rev. B **50**, 5528 (1994).
[25] L. D. Landau and E. M. Lifshitz, *Quantum Mechanics* (Butterworth-Heinemann, Amsterdam, 1981), Vol. 3, pp. 195–198.
[26] W. D. Oliver, Y. Yu, J. C. Lee, K. K. Berggren, L. S. Levitov, and T. P. Orlando, Science **310**, 1653 (2005).
[27] M. Mark, T. Kraemer, P. Waldburger, J. Herbig, C. Chin, H.-C. Nägerl, and R. Grimm, Phys. Rev. Lett. **99**, 113201 (2007).
[28] S. Shevchenko, S. Ashhab, and F. Nori, Phys. Rep. **492**, 1 (2010).
[29] M. Moskalets and M. Büttiker, Phys. Rev. B **66**, 205320 (2002).
[30] L. P. Kouwenhoven, D. G. Austing, and S. Tarucha, Rep. Prog. Phys. **64**, 701 (2001).
[31] S. Kohler, J. Lehmann, and P. Hänggi, Phys. Rep. **406**, 379 (2005).
[32] L. Arrachea and M. Moskalets, Phys. Rev. B **74**, 245322 (2006).
[33] See Supplemental Material at http://link.aps.org/supplemental/10.1103/PhysRevLett.109.216801 for connection of Eqs. (1)–(3) to Floquet theory results of Ref. [23], derivation of τ_{mem} and Eq. (4), and a quantitative estimate of effects due to an additional localized state.
[34] M. Grifoni and P. Hänggi, Phys. Rep. **304**, 229 (1998).
[35] M. Moskalets, P. Samuelsson, and M. Büttiker, Phys. Rev. Lett. **100**, 086601 (2008).
[36] F. Battista and P. Samuelsson, Phys. Rev. B **83**, 125324 (2011).
[37] B. Kaestner, V. Kashcheyevs, S. Amakawa, M. D. Blumenthal, L. Li, T. J. B. M. Janssen, G. Hein, K. Pierz, T. Weimann, U. Siegner *et al.*, Phys. Rev. B **77**, 153301 (2008).
[38] S. P. Giblin, S. J. Wright, J. D. Fletcher, M. Kataoka, M. Pepper, T. J. B. M. Janssen, D. A. Ritchie, C. A. Nicoll, D. Anderson, and G. A. C. Jones, New J. Phys. **12**, 073013 (2010).
[39] G. Yamahata, K. Nishiguchi, and A. Fujiwara, Appl. Phys. Lett. **98**, 222104 (2011).
[40] M. Ya. Azbel', Europhys. Lett. **18**, 537 (1992).
[41] $H_{12} \propto V^2(t)$ since it is a second-order process for electrons in the lead.
[42] C. W. J. Beenakker, Phys. Rev. B **44**, 1646 (1991).